Structural Engineering and Mechanics, Vol. 42, No. 3 (2012) 291-311
DOI: http://dx.doi.org/10.12989/sem.2012.42.3.291

The characteristics of the multi-span suspension bridge with double main cables in the vertical plane

Li-wen Zhang*, Ru-cheng Xiao, Yang Jiang and Sheng-bo Chai

Department of bridge Engineering, Tongji University, 1239 Siping Rd., Shanghai 200092, China

(Received August 30, 2011, Revised January 9, 2012, Accepted March 13, 2012)

Abstract. The multi-span suspension bridge having double main cables in the vertical plane is investigated regarding endurance of live load distribution in the case of non-displaced pylon and pylon displacement. The coefficient formula of live load distribution described as the ratio of live load on the bottom cable to the top cable is obtained. Based on this formula, some function in respect of this bridge are derived and used to analyze its characteristics. This analysis targets the cable force, the cable sag and the horizontal displacement at the pylon top under live load etc. The results clarified that the performance of the live load distribution and the horizontal force of cables in the case of non-deformed pylon has a similar tendency to those in the case of deformed pylon, and the increase of pylon rigidity can increase live load distributed to the bottom cable and slightly raise the cable horizontal force under live load. However, effect on the vertical rigidity of bridge and the horizontal force increment of cables caused by live load is different in the case of non-deformed pylon and deformed pylon.

Keywords: suspension bridge; double main cables; coefficient of live load distribution; cable sag

1. Introduction

At present, the bridge having single main span, both cable-stayed bridge and suspension bridge, hardly cross a strait with wide width over dozens of kilometers like Messina Strait in Italy and Qiongzhou Strait in China, however, their bridging capacity have been improved through innovations of their system (Tan 2009, Zhang 2011a, b, c). A multi-span suspension bridge is one of the most hopeful and rational ways (Torben 2001, Ge 2006, Choi 2010, Zhang 2010, Ge 2011, Luo 2011, Zhang 2011). This suspended structure, however, is restricted by larger deflection under live load acting in one span (Nazir 1986, Ito 1996, Kitagawa 2001, Jung 2010). One way that offers advantages in overcoming this problem is to add two main cables in the vertical plane between pylons (Giming 1997). Nevertheless, the characteristics of this bridge as a new concept is not well understood, though it has been studied and discussed by Gimsing (1997) assuming the constant total horizontal component of the two cables tension.

This paper discusses the rationality of Gimsing's assumption first, after which a study about this bridge with double main cables is carried out with two cases of deformed pylon and non-deformed pylon. The analytical formulas are derived based on the Complete Differential Rule and the

*Corresponding author, Ph.D. Candidate, E-mail: dengpaodaxia@163.com

assumption of non-elongated hangers between the two cables, which include: the live load distribution coefficient defined as the ratio of live loads on the bottom cable to the top cable; the deflection of the cable sag; the horizontal displacement at the pylon top and the horizontal component of the cables tension due to live loads. Moreover, some basic parameters of a general suspension are introduced for a parametric study focusing on performance of this bridge subjected to live load by these formulas.

2. Discussion of the Gimsing assumption

Here the Gimsing's assumption is discussed. Fig. 1 shows the side view of multi-span suspension bridge with double main cables in the vertical plane.

If the Gimsing's assumption is correct, there is no horizontal displacement at the pylon top in the case of live load acting in one span due to the constant horizontal component of the cables tension. That means the cable sag varies only depending on elastic deformation itself. Besides, the horizontal force of the top cable and the bottom cable should be decreased and increased due to live load, respectively. Therefore, a conclusion can be deduced that the cable sag decreased for the top cable and increased for the bottom cable due to live loads, just as shown in Fig. 2.

Nevertheless, this phenomenon, the increase of distance between the top cable and the bottom cable, causes the extension and force increase of the hangers between the top and bottom cables. That means the loads acting on the top cable are increased. Accordingly from the equation

$$H = \frac{ql^2}{8f} \tag{1}$$

where H is cable horizontal force, q is loads cable bears, f is cable sag, another conclusion can also

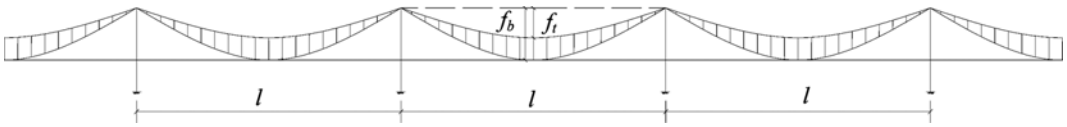

Fig. 1 Side view of multi-span suspension bridge with double main cables in the vertical plane

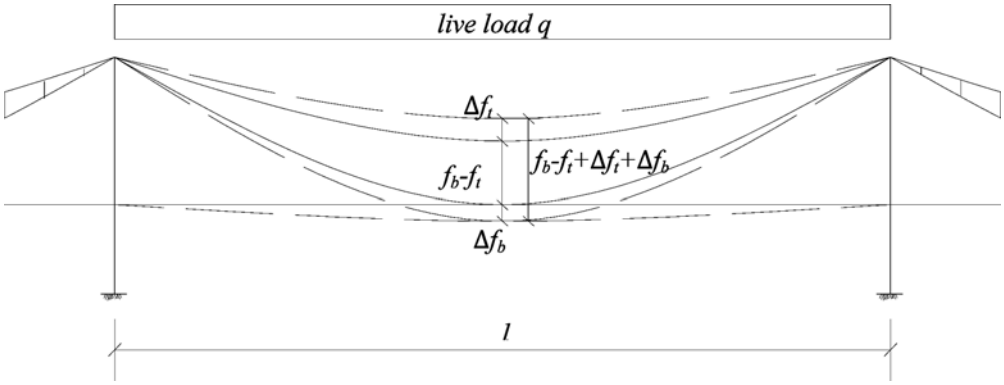

Fig. 2 The condition under live load according to Gimsing assumption

be deduced that the top cable horizontal force increased under live loads. This contradicts to a decrease of the horizontal force of the top cable under live loads as assumption. Thus, the total horizontal force of the top cable and the bottom cable should be variable under live loads on this span.

For this reason, the relative calculation including the live load distribution for two cables, the variation of the cable sag, the horizontal force and the horizontal displacement at the pylon top caused by live loads is carried out in the following sections in the case of deformed pylon and non-deformed pylon.

3. Non-deformed pylon

If the condition of non-deformed pylon called "rigid pylon" stands, meaning the pylon has enough moments of inertia that the pylon cannot bend no matter how much horizontal force the cable has on the pylon top. This suspension bridge can be equivalent to the system as shown in Fig. 3.

In such a case the cable sag varies only depending on the live load-induced elastic deformation. From the equation of cable elongation due to tensile stress

$$s_t = \frac{ql^2}{16fE_cA_c}\left(l + \frac{l^2}{8f}\mathrm{sh}\frac{8f}{l}\right) \tag{2}$$

where q is loads on cable, f is cable sag, l is cable span, E_c is cable elastic modulus, A_c is cable cross section area, the elongation of cable under live load can be expressed as

$$\Delta S = S_t(f_g + \Delta f, g + p) - S_t(f_g, g) \tag{3}$$

where f_g is the cable sag under dead load, g is the dead load, Δf is the increment of cable sag under live load, p is the live load.

According to total differentiation theory, the function

$$\Delta Z = f(x + \Delta x, y + \Delta y) - f(x, y) \tag{4}$$

should be expressed as

$$\Delta Z = \frac{\partial f}{\partial x}\Delta x + \frac{\partial f}{\partial y}\Delta y + \varepsilon_1\Delta x + \varepsilon_2\Delta y \tag{5}$$

where ε_1 is function of Δx, ε_2 is function of Δy, if the partial differential $\partial f/x$ and $\partial f/y$ is continuous in point (x, y). And if Δx and Δy is small enough, the ε_1 and ε_2 are almost zero. The Eq. (6) describes it.

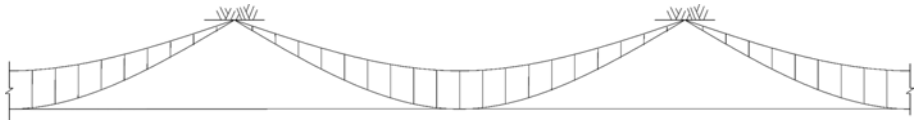

Fig. 3 The bridge with rigid pylon

$$\begin{cases} \Delta Z = \dfrac{\partial f}{\partial x}\Delta x + \dfrac{\partial f}{\partial y}\Delta y \\ \Delta x \to 0, \Delta y \to 0 \end{cases} \tag{6}$$

For Eq. (2), the partial differential for q and f is

$$\begin{cases} \dfrac{\partial S_t}{\partial q} = \dfrac{l^2}{4nE_cA_c}\left(1 + \dfrac{1}{2n}\sinh 2n\right) \\ \dfrac{\partial S_t}{\partial f} = \dfrac{q}{n^2E_cA_c}\left(\cosh 2n - \dfrac{1}{n}\sinh 2n - 1\right) \\ n = \dfrac{4f}{l} \end{cases} \tag{7}$$

of which both are continuous in the point (g, f_g), and, the Δf and p is extremely small against f_g and g. Therefore, the Eq. (3) is equivalent to

$$\begin{cases} \Delta S = \dfrac{l^2\left(1 + \dfrac{1}{2n_0}\sinh 2n_0\right)}{4n_0E_cA_c}p + \dfrac{g\left\{\cosh 2n_0 - \dfrac{1}{n_0}\sinh 2n_0 - 1\right\}}{n_0^2E_cA_c}\Delta f \\ n_0 = \dfrac{4f_g}{l} \end{cases} \tag{8}$$

The curvilinear length of the parabola cable can be calculated using the value of the cable sag and cable span as shown in Eq. (9).

$$s = \frac{l}{2}\left\{\left[1 + 16\left(\frac{f}{l}\right)^2\right]^{1/2} + \frac{\ln\left[\dfrac{4f}{l} + \left[1 + 16\left(\dfrac{f}{l}\right)^2\right]^{1/2}\right]}{\dfrac{4f}{l}}\right\} \tag{9}$$

Then, another function of the cable elongation under loads is obtained

$$\Delta S = S(f + \Delta f) - S(f) \tag{10}$$

Because the differential for f

$$\frac{dS}{df} = 2\frac{n(1+n^2)^{1/2} - \ln[n + (1+n^2)^{1/2}]}{n^2} \tag{11}$$

is also continuous in point (f_g, g), the Eq. (9) is converted to

$$\Delta S = 2\frac{n_0(1+n_0^2)^{1/2} - \ln[n_0 + (1+n_0^2)^{1/2}]}{n_0^2}\Delta f \tag{12}$$

The increment of the cable sag caused by live loads is obtained relying on making Eq. (8) and

Eq. (12) equal. It is expressed as

$$\Delta f = \frac{n_0 l^2\left(1+\frac{1}{2n_0}\sinh 2n_0\right)p}{8E_cA_c\{n_0(1+n_0^2)^{1/2}-\ln[n_0+(1+n_0^2)^{1/2}]\}-4g\left\{\cosh 2n_0-\frac{1}{n_0}\sinh 2n_0-1\right\}} \tag{13}$$

After the substitution of the parameters of the bridge into Eq. (13), the increment of the top and the bottom cable sag is as follows

$$\begin{cases} \Delta f_t = \dfrac{n_{0t} l^2\left(1+\frac{1}{2n_{0t}}\sinh 2n_{0t}\right)p_t}{8E_{ct}A_{ct}\{n_{0t}(1+n_{0t}^2)^{1/2}-\ln[n_{0t}+(1+n_{0t}^2)^{1/2}]\}-4g_t\left\{\cosh 2n_{0t}-\frac{1}{n_{0t}}\sinh 2n_{0t}-1\right\}} \\ n_{0t} = \dfrac{4f_{gt}}{l} \\ \Delta f_b = \dfrac{n_{0b} l^2\left(1+\frac{1}{2n_{0b}}\sinh 2n_{0b}\right)p_b}{8E_{cb}A_{cb}\{n_{0b}(1+n_{0b}^2)^{1/2}-\ln[n_{0b}+(1+n_{0b}^2)^{1/2}]\}-4g_b\left\{\cosh 2n_{0b}-\frac{1}{n_{0b}}\sinh 2n_{0b}-1\right\}} \\ n_{0b} = \dfrac{4f_{gb}}{l} \end{cases} \tag{14}$$

where f_{gb} is the bottom cable sag under dead load, f_{gt} is the top cable sag under dead load; Δf_t is the top cable sag change, Δf_b is the bottom cable sag change; g_d is the dead load on the bottom cable, g_t is the dead load on the top cable; E_{ct} is the top cable elastic modulus, E_{cb} is the bottom cable elastic modulus; A_{ct} is the top cable cross section area, A_{cb} is the bottom cable cross section area.

Accordingly, the coefficient β of live load distribution described as the ratio of live loads on the bottom cable to the top cable can be derived based on assuming that the hanger is not elongated, that is, $\Delta f_t = \Delta f_b$. It is expressed as

$$\beta = \frac{p_d}{p_t} = \frac{J(n_{0t})[E_{cd}A_{cd}G(n_{0b})-g_bF(n_{0b})]}{J(n_{0b})[E_{ct}A_{ct}G(n_{0t})-g_tF(n_{0t})]} \tag{15}$$

where $J(x)$, $F(x)$ and $G(x)$ respectively is a function of x. these are shown in Eq. (16).

$$\begin{cases} G(x) = 8\cdot\{x(1+x^2)^{1/2}-\ln[x+(1+x^2)^{1/2}]\} \\ F(x) = 4\left\{\cosh 2x-\dfrac{1}{x}\sinh 2x-1\right\} \\ J(x) = x\left(1+\dfrac{1}{2x}\sinh 2x\right) \end{cases} \tag{16}$$

From Eq. (15) and Eq. (16), the live load acting on the top cable and the bottom cable respectively can be calculated by introducing β into Eq. (17).

$$\begin{cases} p_t = \dfrac{1}{1+\beta} p \\ p_b = \dfrac{\beta}{1+\beta} p \end{cases} \tag{17}$$

where p is the total of live loads on bridge. These may be used to deduce the increment of cable sag Δf by Eq. (14), the increment of cable horizontal force including the top cable ΔH_t, the bottom cable ΔH_b, and the total cable horizontal force ΔH by Eq. (18).

$$\begin{cases} \Delta H_t = \dfrac{(g_t + p_t) l^2}{8(f_{gt} + \Delta f)} - \dfrac{g_t l^2}{8 f_{gt}} \\ \Delta H_b = \dfrac{(g_b + p_b) l^2}{8(f_{gb} + \Delta f)} - \dfrac{g_b l^2}{8 f_{gb}} \\ \Delta H = \Delta H_t + \Delta H_b \end{cases} \tag{18}$$

4. Deformed pylon

The pylon of a suspension bridge, in practice, does not usually have such a large moments of inertia keeping from its deflection when live load is on one side of spans. Thus, the displacement of pylon top must be taken into consideration in the calculation of suspension bridge. Fig. 4 describes this condition.

For a multi-span suspension bridge, the increment of the cable horizontal force caused by live loads can be described as the combined value of the horizontal displacement at the pylon top and the horizontal displacement rigidity coefficient, as follows

$$\Delta H = K \Delta l \tag{19}$$

where Δl is the horizontal displacement at the pylon top; K is the horizontal displacement rigidity coefficient consisting of the pylon and the cable in the adjacent span, as follows

$$K = K_c + K_p \tag{20}$$

where K_p is the bending rigidity coefficient of the pylon, K_c is the rigidity coefficient of the cable

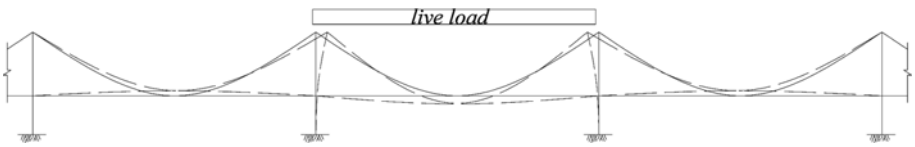

Fig. 4 The bridge with the displacement of pylon top

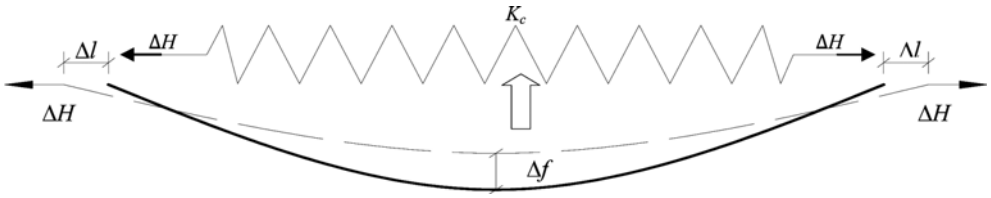

Fig. 5 The rigidity of the cable displacement in the horizontal direction

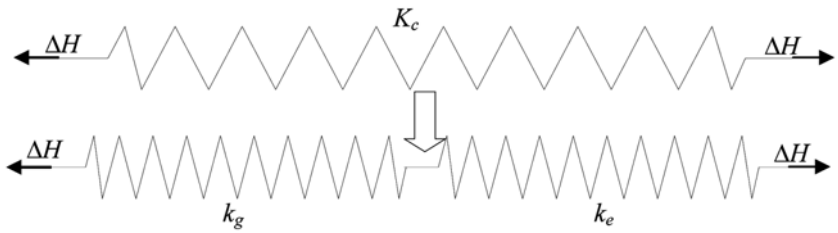

Fig. 6 The simplified calculation model of K_c

displacement in the horizontal direction in the adjacent span of the loaded span as shown in Fig. 5.

It can be easy to come to the K_p, as follows

$$K_p = 3E_pI_p/h_p^3 \tag{21}$$

where E_p is the pylon elastic modulus, I_p is the pylon moments of inertia, h_p is the pylon height. Nevertheless, the calculation of the K_c is complex due to the fact that it includes two parts of the displacement, that is, the displacement from the cable elastic extension and the displacement from the cable profile distortion. In order to obtain a highly precise and simple form equation for K_c, the rigidity coefficient of the cable displacement in the horizontal direction is converted to a combined system of two springs connected in series. One is the spring with the rigidity coefficient k_g resisting geometry deformation; another is the spring with the rigidity coefficient k_e resisting elastic deformation, just as shown in Fig. 6.

The value of K_c is obtained from Eq. (22).

$$K_c = \frac{k_g k_e}{k_g + k_e} \tag{22}$$

where k_e is the function with respect to the material properties of the cable, as follows

$$k_e = E_c A_c / l_g \tag{23}$$

where l_g is the span of the cable before live load acting on bridge, and the derived process of the k_g is shown in the following contents.

As for the horizontal force increment of the cable in non-loaded span, the factors that concern it are the increment of the cable sag and the cable span because that this increment of the cable horizontal force are only caused by the cable profile distortion due to the cable tension pull from the loaded span, as follows

$$\Delta H = H(l+\Delta l, f+\Delta f) - H(l,f) \tag{24}$$

where l is the cable span, Δl is the increment of the cable span; f is the cable sag, Δf is the increment of the cable sag. The partial differential of Eq. (1) for l and f is expressed as

$$\begin{cases} \dfrac{\partial H}{\partial l} = \dfrac{ql}{4f} \\ \dfrac{\partial H}{\partial f} = -\dfrac{ql^2}{8f^2} \end{cases} \tag{25}$$

of which the both are continuous in the point (g, l_g, f_g), in the same way Eq. (24) also can be written by performing the Complete Differential Rule as

$$\Delta H = \frac{gl_g}{4f_g}\Delta l - \frac{gl_g^2}{8f_g^2}\Delta f = g\left(\frac{l_g}{4f_g} - \frac{l_g^2}{8f_g^2}\frac{\Delta f}{\Delta l}\right)\Delta l \tag{26}$$

where g is the dead load on the cable, f_g is the cable sag under dead load. Due to ignoring the elastic elongation of the cable, the variation of the cable curvilinear length must be zero

$$\Delta S(l,f) = S(l+\Delta l, f+\Delta f) - S(l,f) = 0 \tag{27}$$

The partial differential of Eq. (9) for l and f, as follows

$$\begin{cases} \dfrac{\partial S(f,l)}{\partial f} = 2\dfrac{n(1+n^2)^{1/2} - \ln[n+(1+n^2)^{1/2}]}{n^2} \\ \dfrac{\partial S(f,l)}{\partial l} = \dfrac{\ln[n+(1+n^2)^{1/2}]}{n} \\ n = \dfrac{4f}{l} \end{cases} \tag{28}$$

are also continuous in the point (g, l_g, f_g) so that Eq. (26) is converted to Eq. (29).

$$\begin{cases} \Delta S = 2\dfrac{n(1+n_0^2)^{1/2} - \ln[n_0+(1+n_0^2)^{1/2}]}{n_0^2}\Delta l + \dfrac{\ln[n_0+(1+n_0^2)^{1/2}]}{n_0}\Delta f = 0 \\ n_0 = \dfrac{4f_g}{l_g} \end{cases} \tag{29}$$

From Eq. (29), the ($\Delta f/\Delta l$) can be derived, as follows

$$\frac{\Delta f}{\Delta l} = \frac{n_0 \ln[n_0+(1+n_0^2)^{1/2}]}{2\{\ln[n_0+(1+n_0^2)^{1/2}] - n_0(1+n_0^2)^{1/2}\}} \tag{30}$$

which is the same as (df/dl) derived by Osamu Yoshida (2004). After the substitution of Eq. (30) in Eq. (26), the k_g is obtained

$$k_g = \frac{\Delta H}{\Delta l} = \frac{g(1+n_0^2)^{1/2}}{n_0(1+n_0^2)^{1/2} - \ln[n_0 + (1+n_0^2)^{1/2}]} \tag{31}$$

Then, the K_c and K can be calculated, as follows

$$\begin{cases} K_c = \dfrac{g(1+n_0^2)^{1/2} E_c A_c}{g l_g (1+n_0^2)^{1/2} + E_c A_c \{n_0(1+n_0^2)^{1/2} - \ln[n_0 + (1+n_0^2)^{1/2}]\}} \\ K = \dfrac{3E_p I_p}{h_p^3} + \dfrac{g(1+n_0^2)^{1/2} E_c A_c}{g l_g (1+n_0^2)^{1/2} + E_c A_c \{n_0(1+n_0^2)^{1/2} - \ln[n_0 + (1+n_0^2)^{1/2}]\}} \end{cases} \tag{32}$$

Based on replacing the parameters in Eq. (32) by the parameters of the double main cables suspension bridge, the K_c and K of this bridge can be obtained

$$\begin{cases} K_c = \dfrac{g_s(1+n_{0s}^2)^{1/2} E_{cs} A_{cs}}{g_s l_{gs} (1+n_{0s}^2)^{1/2} + E_{cs} A_{cs} \{n_{0s}(1+n_{0s}^2)^{1/2} - \ln[n_{0s} + (1+n_{0s}^2)^{1/2}]\}} \\ K = \dfrac{3E_p I_p}{h_p^3} + \dfrac{g_s(1+n_0^2)^{1/2} E_{cs} A_{cs}}{g_s l_{gs} (1+n_{0s}^2)^{1/2} + E_{cs} A_{cs} \{n_{0s}(1+n_{0s}^2)^{1/2} - \ln[n_{0s} + (1+n_{0s}^2)^{1/2}]\}} \\ n_{0s} = \dfrac{4f_{gs}}{l_{gs}} \end{cases} \tag{33}$$

where g_s is the total dead load, E_{cs} is the elastic modulus of the cables; A_{cs} is the total section area of the top and the bottom cable; l_{gs} is the span of the cable in the adjacent span of the loaded span, f_{gs} is the equivalent sag of the cables under dead load derived from the following.

The total horizontal force of the adjacent span cables can be derived by Eq. (1), as follows

$$H_{gs} = \frac{g_{st} l_{gs}^2}{8 f_{gst}} + \frac{g_{sb} l_{gs}^2}{8 f_{gsb}} \tag{34}$$

where g_{st} and g_{sb} is the dead load on the top and the bottom cable, f_{gst} and f_{gsb} is the sag of the top and the bottom cable under dead load. Set $\alpha_s = g_{sb}/g_{st}$, Eq. (34) is converted to Eq. (35)

$$H_{gs} = \frac{g_s l_{gs}^2 (f_{gsb} + \alpha_s f_{gst})}{8 f_{gst} f_{gsb} (1 + \alpha_s)} \tag{35}$$

which has structural similarities to Eq. (1), so the f_{gs} is expressed as

$$f_{gs} = \frac{f_{gst} f_{gsb} (1 + \alpha_s)}{(f_{gsb} + \alpha_s f_{gst})} \tag{36}$$

As for the span applied by live loads, the entire cable span, the cable sag and the load are variable. So the variation of the cable horizontal force can be written by a function including the increment of the cable span, the cable sag and the load

$$\Delta H = H(l + \Delta l, q + \Delta q, f + \Delta f) - H(l, q, f) \tag{37}$$

where l is the cable span, q is the load, f is the cable sag; Δl, Δq and Δf respectively is the increment of the l, q and f. The partial differential of Eq. (1) for l, q and f is expressed as

$$\begin{cases} \dfrac{\partial H(f,l,q)}{\partial f} = -\dfrac{gl^2}{8f^2} \\ \dfrac{\partial H(f,l,q)}{\partial l} = 2\dfrac{gl}{8f} \\ \dfrac{\partial H(f,l,q)}{\partial q} = \dfrac{l^2}{8f} \end{cases} \tag{38}$$

all of which are continuous in the point (g_m, l_{gm}, f_{gm}), Eq. (37) can be converted to Eq. (39), as follows

$$\Delta H = 2\frac{g_m l_{gm}}{8f_{gm}}\Delta l_m + \frac{l_{gm}^2}{8f_{gm}}p - \frac{g_m l_{gm}^2}{8f_{gm}^2}\Delta f_m \tag{39}$$

where g_m is the dead load, l_{gm} is the cable span under dead load, f_{gm} is the cable sag under dead load; Δl_m, Δf_m respectively is the increment of the cable span and cable sag due to live load, p is the live load. The increment of the cable horizontal force due to live loads, from Eq. (19), is the combined value of K and Δl. Here Δl is the displacement of the pylon top equaling to minus one-half of Δl_m. Thus, Eq. (39) is converted to

$$K = -\frac{g_m l_{gm}}{2f_{gm}} - \frac{l_{gm}^2}{4f_{gm}}\frac{p}{\Delta l_m} + \frac{g_m l_{gm}^2}{4f_{gm}^2}\frac{\Delta f_m}{\Delta l_m} \tag{40}$$

The live load-induced elastic elongation of the cable is negligible; the function of Δl_m and Δf_m can be obtained by the same way of calculating k_g, as follows

$$\begin{cases} \dfrac{\Delta f_m}{\Delta l_m} = \dfrac{n_{m0}\ln[n_{m0} + (1+n_{m0}^2)^{1/2}]}{2\{n_{m0}(1+n_{m0}^2)^{1/2} - \ln[n_{m0} + (1+n_{m0}^2)^{1/2}]\}} \\ n_{m0} = \dfrac{4f_{gm}}{l_{gm}} \end{cases} \tag{41}$$

Therefore, using Eq. (40) and Eq. (41), the increment of the cable sag caused by live load can be calculated by

$$\Delta f_m = \frac{l_{gm}\ln[n_{m0} + (1+n_{m0}^2)^{1/2}]}{4\left\{\{n_{m0}(1+n_{m0}^2)^{1/2} - \ln[n_{m0} + (1+n_{m0}^2)^{1/2}]\}\dfrac{K}{2} + g_m(1+n_{m0}^2)^{1/2}\right\}}p \tag{42}$$

The coefficient β of live load distribution is obtained by the same way of deriving β, Eq. (15), in the case of non-deformed pylon, as follows

$$\begin{cases} \beta = \dfrac{\ln[n_{mt0}+(1+n_{mt0}^2)^{1/2}]\left\{\dfrac{\{n_{mb0}(1+n_{mb0}^2)^{1/2}-\ln[n_{mb0}+(1+n_{mb0}^2)^{1/2}]\}K}{2}+g_{mb}(1+n_{mb0}^2)^{1/2}\right\}}{\ln[n_{mb0}+(1+n_{mb0}^2)^{1/2}]\left\{\dfrac{\{n_{mt0}(1+n_{mt0}^2)^{1/2}-\ln[n_{mt0}+(1+n_{mt0}^2)^{1/2}]\}K}{2}+g_{mt}(1+n_{mt0}^2)^{1/2}\right\}} \\ n_{mt0}=\dfrac{4f_{gmt}}{l_{gm}}, \quad n_{mb0}=\dfrac{4f_{gmb}}{l_{gm}} \end{cases} \tag{43}$$

where f_{gmt} is the top cable sag under dead load, f_{gmb} is the bottom cable sag under dead load, g_{mb} is the dead load on the bottom cable, g_{mt} is the dead load on the top cable. And the live load acting on the top cable and the bottom cable, the increment of cable horizontal force, the increment of cable sag Δf_m and the displacement of the pylon are calculated by Eq. (17), Eq. (44), and Eq. (42), Eq. (19), respectively.

$$\begin{cases} \Delta H_t = \dfrac{(g_{mt}+p_t)(l_{gm}+\Delta l_{gm})^2}{8(f_{gmt}+\Delta f_m)}-\dfrac{g_{mt}l_{gm}^2}{8f_{gmt}} \\ \Delta H_b = \dfrac{(g_{mb}+p_b)(l_{gm}+\Delta l_m)^2}{8(f_{gmb}+\Delta f_m)}-\dfrac{g_{mb}l_{gm}^2}{8f_{gmb}} \\ \Delta H = \Delta H_t+\Delta H_b \end{cases} \tag{44}$$

5. The characteristics of the bridge

5.1 Basic parameters

In order to understand the characteristics of the multi-span suspension bridge with double main cables in the vertical plane, the following parameters of a general suspension bridge are introduced

Table 1 Basic parameters

Parameters	Contents	Values
E_c	Cable elastic modulus	2.06×10^{11} (Pa)
E_p	Pylon elastic modulus	2.06×10^{11} (Pa)
A_{ct}, A_{cb}	Top cable area and bottom cable area	0.669 (m^2)
f_{gt}, f_{gst}, f_{gmt}	Top cable sag under dead load	50 (m)
f_{gb}, f_{gsb}, f_{gmb}	Bottom cable sag under dead load	100 (m)
l, l_{gs}, l_{gm}	Bridge span and cable span under dead load	1000 (m)
I_p	Pylon inertia moment	13.7944 (m^4)
h_p	Pylon height	125 (m)
g	Total dead load of each span	2.65×10^5 (N/m)
γ_c	Cable volume-weight	85 (kN/m^3)

into the formulas derived in this paper, which include the cable elastic modulus, the cable area, the pylon height, the span, and the dead and live load etc. In addition, the basic parameters per one span are the same, as shown in Table 1.

5.2 Formula verification

In order to verify the correctness of this formula, a spatial element model is established for simulation. Spatial beam element is used for the girder and the pylons, and cable element is adopted for the main cables and suspenders. This model is of five main spans and basic parameters shown in Table 1. Fig. 7 is the side view of this model. After the simulation, the simulated value will be compared with the calculated value.

Fig. 8 shows the deflection as load varying calculated by formula and numerical simulation, respectively. In Fig. 8, red line shows the simulated value and blue line shows the calculated value. Besides, the error between them is also presented in Fig. 9.

In the region of where live load = 13 kN/m, 19.6 kN/m, 26.1 kN/m, 32.6k N/m and 39.1 kN/m, the error is 4.07%, 4.12%, 4.28%, 4.42% and 4.52%, respectively. This shows that the error of this formula increases as increasing of live load. However, the maximum error is still less than 5%, which means that the accuracy of the formula is acceptable in the region of general live load acting on bridge.

The error of this formula may be caused by the negligible elastic elongation of suspenders between two cables and the simplified rigidity coefficient of the cable horizontal displacement comprised of two springs connected in series.

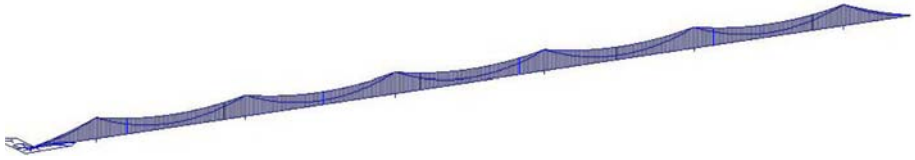

Fig. 7 The side view of model

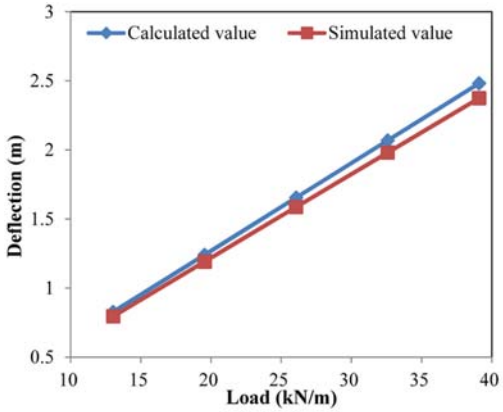

Fig. 8 The value of calculation and simulation

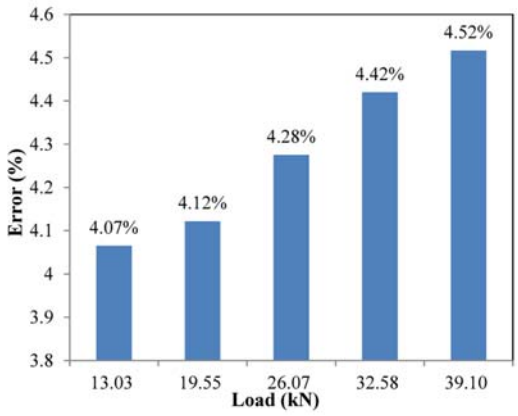

Fig. 9 The error

5.3 The characteristics of the bridge with rigid pylon

The ratio of the dead load on the bottom cable to the total dead load called "α_b" is induced as an index for recognizing the characteristics of the bridge

$$\alpha_b = \frac{g_b}{g} \tag{45}$$

The research targets the coefficient of the live load distribution, the increment of sag, and the horizontal force and its increment of cables due to live loads.

Fig. 10 shows the influences of α_b on targets. The α_b ranges from 0.1 to 0.9.

The coefficient of the live load distribution, from Fig. 10, is increasing with the increase of α_b, which means that the more dead load there is on the bottom cable, the more live load there is on it. The influence of α_b on the increment of cable sag and on the coefficient of the live load distribution shows a similar tendency. The magnitude above targets, however, changes slightly with an increase in α_b, and this shows that the distribution of live load on cables and the increment of the cable sag are basically independent of dead load applied at the cable possibly because of the negligible elongation of cables.

The total horizontal force increment of cables increases with raising the coefficient α_b due to the

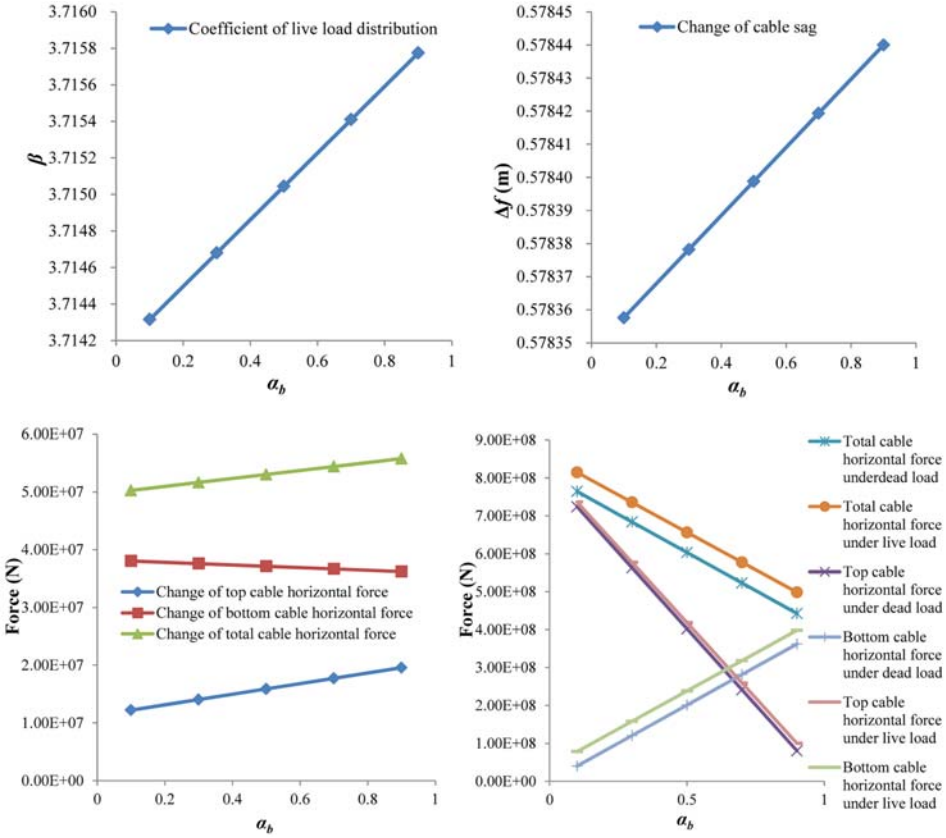

Fig. 10 The influences of α_b

increased horizontal force increment of the top cable and the constant horizontal force increment of the bottom cable.

The total horizontal force of two cables after live load acting, however, shows a declining tendency. That's because although the bottom cable horizontal force under dead load is increasing, the total horizontal force under dead load decreases for higher α_b as the horizontal force of the top cable declines faster than of the bottom cable grows. Similarly, the horizontal force of the top cable after live load acting is decreasing caused by its falling under dead load. By contrast, the horizontal force of the bottom cable under live load increases with the increase of α_b because of its growth under dead load.

Fig. 11 offers the influence of the bottom cable sag under dead load rising from 75 m to 115 m. An effect on the live load distribution similar to but more serious than Fig. 10 can be observed. The increase of the bottom sag under dead load decreases the deflection of the cable due to live load (the increment of the cable sag), and this means that can raise the stiffness of bridge.

The entire the horizontal force increment of the top cable, the bottom cable and the total cable are falling with the increasing of the bottom cable sag under dead load. In addition, the increment of the bottom cable horizontal force declines gently.

Both of the total cable and the bottom cable horizontal force caused by dead load are reduced by the increase of the bottom cable sag under dead load. Hence their horizontal force under live load

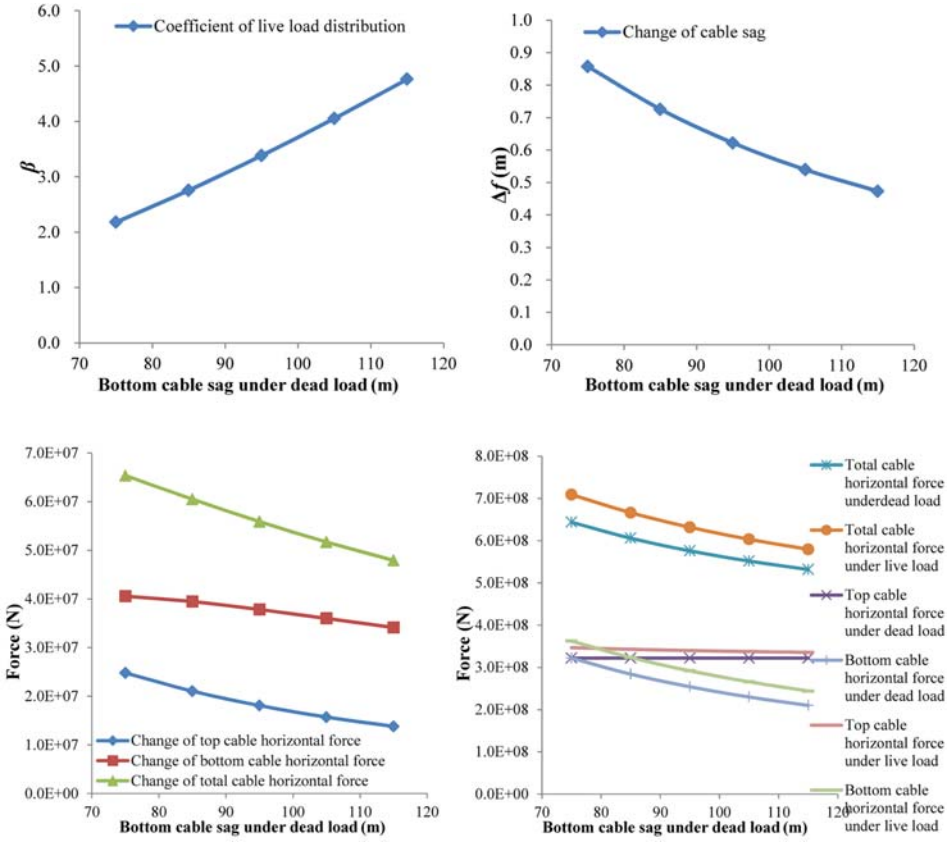

Fig. 11 The influences of the bottom cable sag under dead load

decreases while its increment also declines. As for the horizontal force of the top cable under live load, it represents a tendency with constant horizontal force because of its negligible increase under dead load and the decline of its increment caused by live load with raising the bottom cable sag under dead load.

Fig. 12 describes the influence of the top cable sag under dead load ranging from 30 m to 70 m. The coefficient of the live load distribution, in Fig. 12, shows a reverse tendency to Fig. 11. It declines with the increase of the top cable sag under dead load. Nevertheless, the effect on the increment of the cable sag is similar to that of the bottom cable sag under dead load.

The increment of the bottom cable horizontal force decreases for greater top cable sag under dead load, and this tendency is nearly linear. The horizontal force increment of the top cable and the total cable, however, shows an irregularly growth. In the region of the top cable sag under dead load less than 40 m, the greater the top cable sag under dead load is the more increment of the total cable horizontal force is. In the region of the top cable sag under dead load larger than 40 m, it basically keeps constant. Additionally, the slope of the top cable horizontal force increment shows a tendency with declining.

The horizontal force of the total cables and the top cable under live load, however, also decreases because of its decrease under dead load. As for the horizontal force of the bottom cable, it still decreases with raising the top cable sag under dead load in the case of live load acting due to the

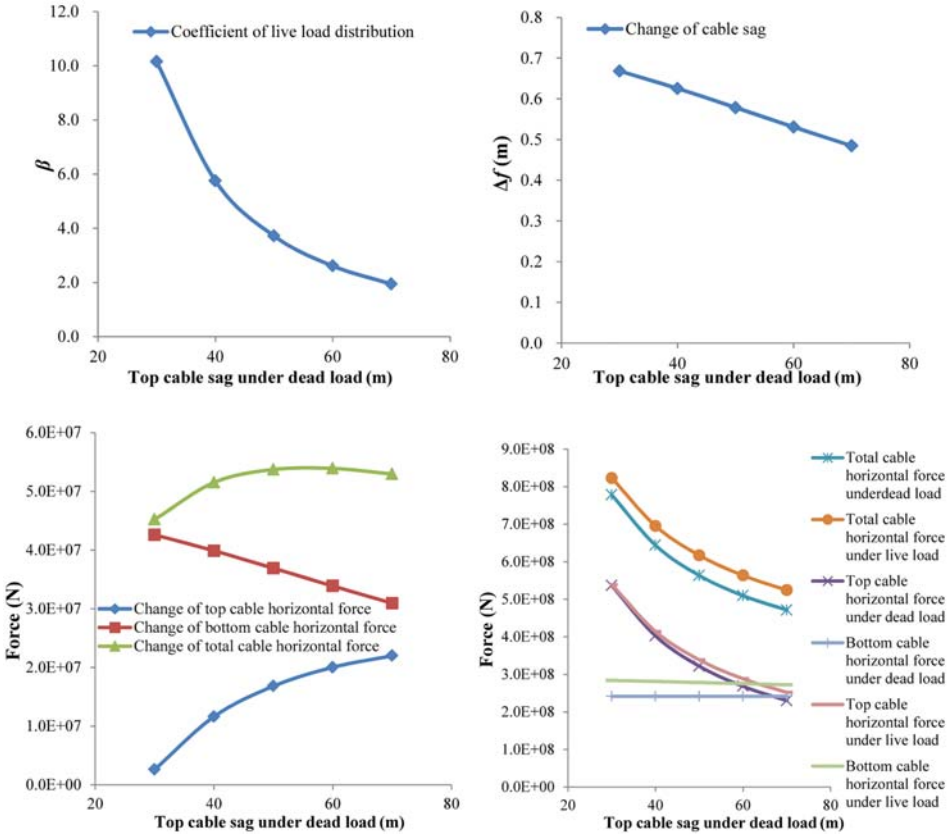

Fig. 12 The influences of the top cable sag under dead load

decrease of its increment caused by live load, although it increases under dead load but slowly.

5.4 Characteristics of the bridge with pylon flexible

The targets of research concerning, the bridge with flexible pylon, include the coefficient of the live load distribution, the increment of sag, the live load-induced cable horizontal force and its increment, and the horizontal displacement at the pylon top.

Fig. 13 shows the influences of α_b varying from 0.1 to 0.9.

The curvilinear increment of β, from Fig. 13, can be observed. In the region where α_b is less than 0.5, the tendency with increasing β is slight, and it becomes prominent when α_b is larger than 0.5. This means that the magnitude of the dead load on cables has a small effect on the live load distribution when the dead load applied at the bottom cable is less than that applied at the top cable, and the tendency of raising live load distributed to the bottom cable caused by an increase of dead load on itself becomes remarkable when the dead load applied at the bottom cable is larger than that applied at the top cable

Due to an increase of the cable sag increment and the horizontal displacement at the pylon top, in Fig. 13, it is evident that raising dead load on the bottom cable lowers the vertical rigidity of the bridge, contrary to the case of non-deformed pylon. That is possibly because distributing more dead load to the bottom cable makes the rigidity coefficient k_g of cables in adjacent span smaller.

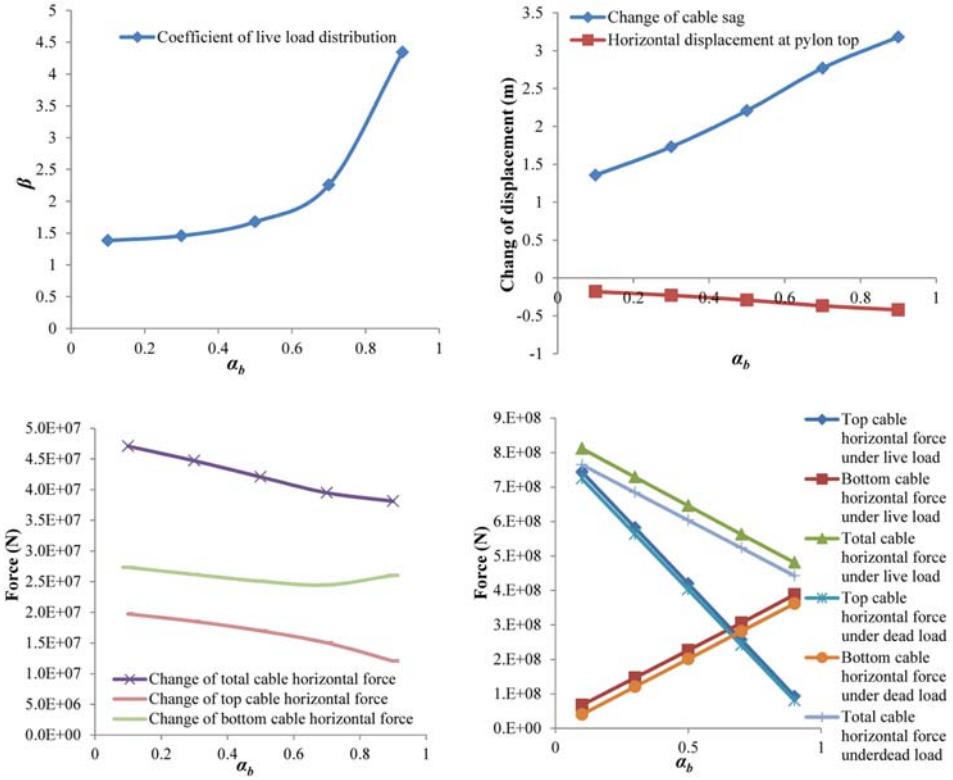

Fig. 13 The influences of α_b

As for the horizontal force increment of the bottom cable, the top cable and the total cable caused by live load, these are lowered by increasing α_b. But in the region of α_b larger than 0.7, the effect on the horizontal force increment of the bottom cable becomes in the opposite direction.

The effect of α_b on the horizontal force of cables shows a similar tendency to the case of non-deformed pylon in Fig. 10.

Fig. 14 offers the influence diagrams of the bottom cable sag under dead load in the region of ranging from 75 m to 115.

The live distribution coefficient shows a straight linear upward tendency with the increase of the bottom cable sag under dead load. That means the lager the bottom cable sag under dead load is, the larger the live load applied at the bottom cable is.

As for the increment of the cable sag caused by live load, it only represent a slightly variation in the region of where the bottom cable sag under dead load ranges from 75 m to 85 m, but becomes a constant value when the bottom cable sag under dead load is larger than 85 m. This clarifies that the bottom cable sag under dead load hardly affects the cable sag increment and the horizontal displacement at the pylon top under live load, that is, it is independent of the vertical rigidity of this bridge.

The horizontal force increment of cables including the total cables, the bottom cable and the top cable shows a decreased tendency with increasing the bottom cable sag under dead load. Additionally, the increment of the bottom cable declines more gently than others.

Fig. 14 shows a gentle variation of the cable horizontal force comparing with Fig. 13; this means

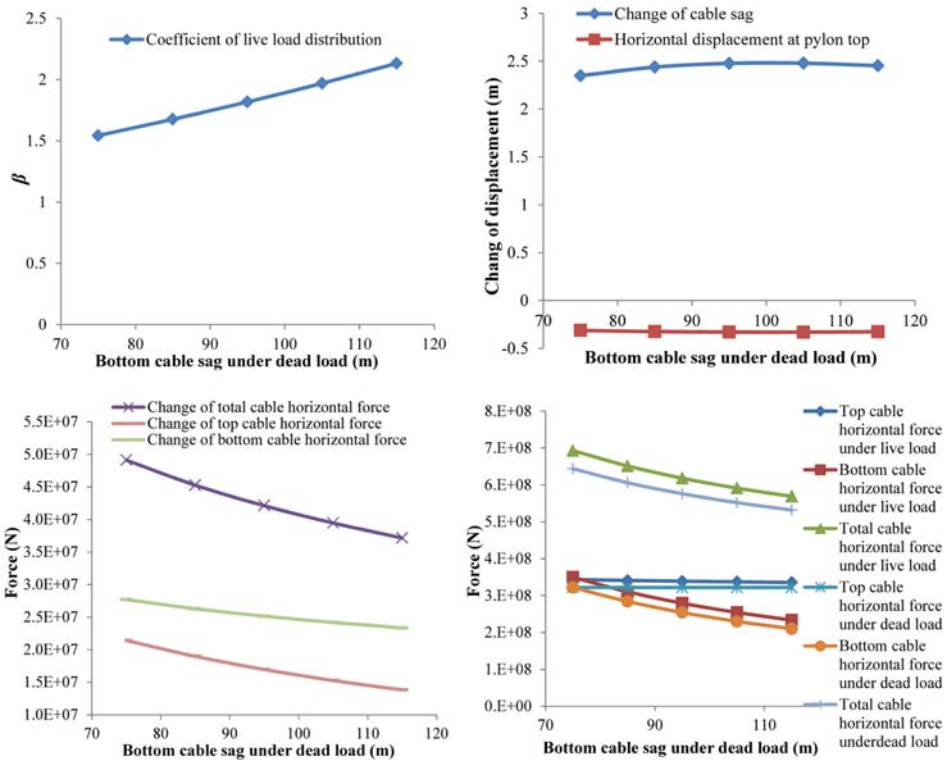

Fig. 14 The influences of the bottom cable sag under dead load

that the bottom cable sag under dead load has less effect on the cable horizontal force than the dead load applied at the bottom cable. The horizontal force of the total cable and the bottom cable caused by live load decreases for larger bottom cable sag under dead load, but the horizontal force of the top cable due to live load basically keeps a constant because of a slower increase of itself under dead load and a decrease of its increment caused by live load.

Fig. 15 shows the influence of the top cable sag under dead load ranging from 30 m to 70 m.

The tendency of β declining with an increase of the top cable sag under dead load is observed, and this means that the growth of the top cable sag under dead load decreases the live load distributed to the bottom cable. The increment of cable sag and the horizontal displacement at the pylon top shows an upward tendency, which is similar to Fig. 13. The slop of the cable sag increment, however, becomes slow gradually; it clarifies that the effect of the top cable sag under dead load on the bridge vertical rigidity is gradually weak when the top cable sag under dead load becomes larger.

As for the horizontal force increment of the bottom cable and the total cables caused by live load, it decreases with the increase of the top cable sag under dead load. Additionally, the horizontal force increment of the total cables shows a slower decrease than that of the bottom cable due to a slowly increase of the top cable horizontal force increment caused by live load.

The horizontal force of the total cables shows a decreased tendency with increasing the top cable sag under dead load due to its decrease under dead load and a decrease of its increment under live

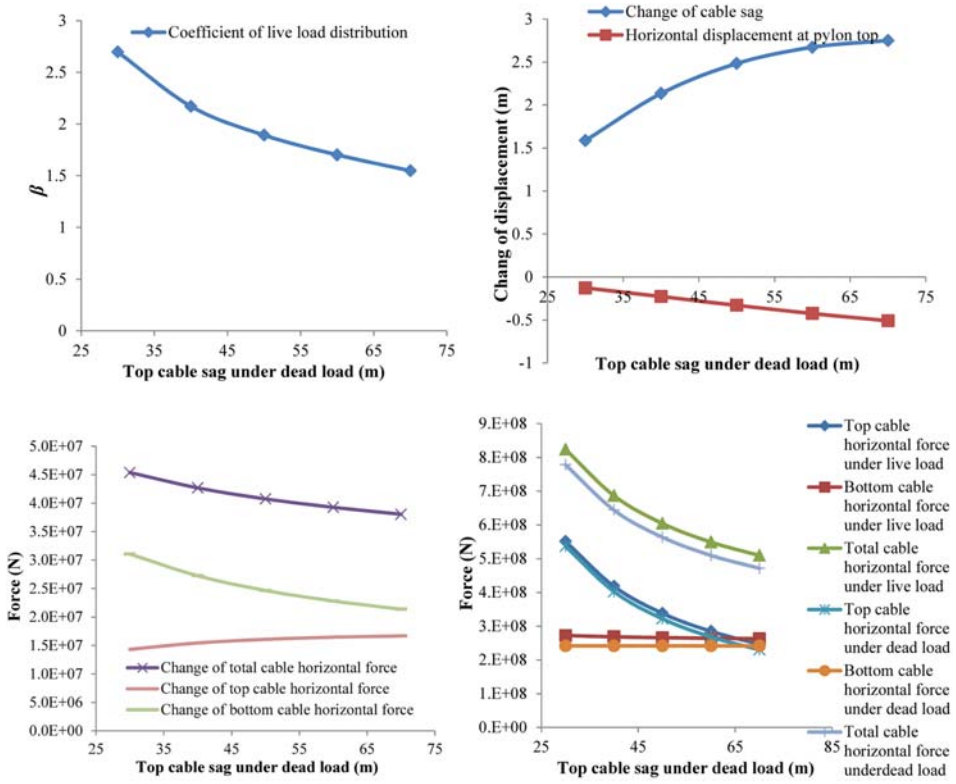

Fig. 15 The influences of the top cable sag under dead load

load. However as described previously, the horizontal force increment of the top cable induced by live load increases for lager top cable sag under dead load, the horizontal force of the top cable under live load still decreases because of its decrease under dead load and a slower increase of its increment under live load. In contrary, the horizontal force of the bottom cable under live load basically remains level due to its slower growth under dead load and a decline of its increment under live load.

Fig. 16 shows the influence of the pylon inertia moment when it ranges from 1 to 16 times as the moments of inertia in Table 1.

A tendency of increasing β with raising pylon inertia moment is observed from Fig. 16. It means that the increase of pylon rigidity can increase the live load distributed to the bottom cable. A conclusion of the vertical rigidity of bridge raised by increasing pylon rigidity can be obtained from Fig. 16 in which both of the cable sag increment and the horizontal displacement at the pylon top decrease with an increase of pylon inertia moment. And when the inertia moment of the pylon is 16 times as the value shown in Table 1, the increment of the cable sag is approximately the value in the case of non-deformed pylon, and the horizontal displacement at the pylon top is approximately zero.

As for the horizontal force of the total cables, the bottom cable and the top cable under dead load, it basically keeps constant, and this means that the cable force under dead load is independent of pylon rigidity. Additionally, the horizontal force of cables under live load slightly increases due to a slower increase of its increment caused by live load in Fig. 16.

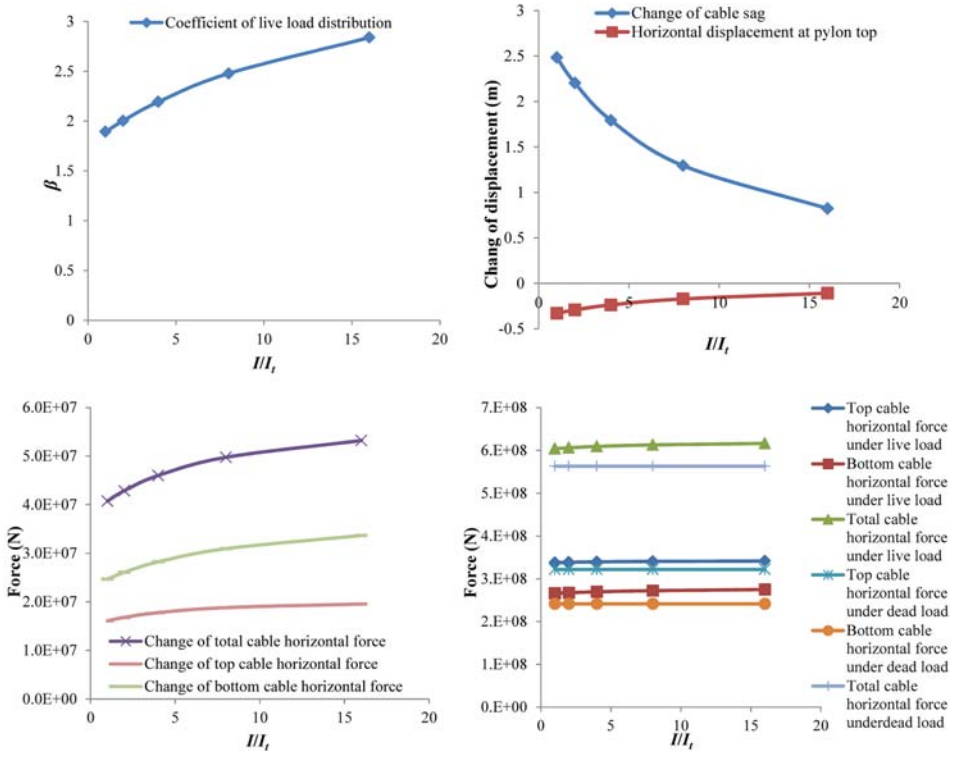

Fig. 16 The influences of the pylon inertia moment

6. Conclusions

The analytical formulas in respect of multi-span suspension bridge with double main cables in the vertical plane have been derived in this paper, which include the live load distributed between two cables, and the horizontal force, its increment, and the sag increment of cables under live load. Based on these analytical formulas, the characteristics of this bridge have been investigated, and the major conclusion can be summarized as

1. In the case of rigidity pylon, the distribution of live load between two cables is in respect of the dead load distributed to cables and the distance between two cables. The larger dead load distributed to the bottom cable and the larger distance, the larger live load distributed to the bottom cable becomes. This is similar to the case with deformed pylon. Moreover, higher pylon rigidity can increase live load distributed to the bottom cable.
2. The bridge vertical stiffness shows a different performance in the case of rigid pylon and flexible pylon. In the case of rigid pylon, the increase of the bridge vertical stiffness is in proportion to dead load distributed to the bottom cable and the sag of cable under dead load. But in the case of flexible pylon, it is inversely proportional to dead load distributed to the bottom cable and the sag of the top cable, and in proportion to the pylon rigidity.
3. The characteristics of the cable horizontal force increment, in the case of rigid pylon, also differ from the case of flexible pylon. The horizontal force increment of the top cable and the total cables, in the case of rigid pylon, is inversely proportional to the dead load distributed to the top cable and the distance between two cables, and the horizontal force increment of the bottom cable varied inversely as the dead load on itself and its sag under dead load. Nevertheless in the case of flexible pylon, the horizontal force increment of the bottom and the total cable is inversely proportional to the dead load distributed to the bottom cable and the bottom cable sag under dead load, and the horizontal force increment of the top cable varied inversely as the dead load on the bottom cable and the distance between two cables. Moreover, the entire horizontal force increment of cable is raised by increasing pylon rigidity.
4. Regardless of whether pylon is rigid or flexible, the horizontal force of two cables increases inversely as their sag under dead load and directly as dead load distributed to them, and the horizontal force of the total cables is inversely proportion to cable sag under dead load and dead load distributed to the bottom cable. As for the case of deformed pylon, increasing pylon rigidity hardly affects the horizontal force of cables under dead load but slightly increase the horizontal force of cables under live load.

References

Choi, D.H., Na, H.S., Gwon, S.G., Yoo, D.H. and Moon, C. (2010), "A parametric study on the ultimate behaviors of multi-span suspension bridges", *Proceedings of 34th International Symposium on Bridge and Structural Engineering*, Venice, September.

Ge, Y.J. and Xiang, H.F. (2006), "Tomorrow's challenge in bridge span length", *Proceedings of IABSE Symposium on Responding to Tomorrow's Challenges in Structural Engineering*, Budapest, September.

Ge, Y.J. and Xiang, H.F. (2011), "Extension of bridging capacity of cable-supported bridges using double main spans or twin parallel decks solutions", *Struct. Infras. Eng.*, **7**(7-8), 551-567.

Giming, N.J. (1997), *Cable Supported Bridges-Concept & Design*, Willey, New York.

Ito, M. (1996), "Cable-supported steel bridges: design problems and solutions", *J. Constr. Steel. Res*., **39**(1), 69-84.

Jung, J., Kim, J., Baek, J. and Choi, H. (2010), "Practical design of continuous two main-span suspension bridge in Korea", *Proceedings of 34th International Symposium on Bridge and Structural Engineering*, Venice, September.

Kitagawa, M., Kashima, N., Fukunaga, S. and Anzar, M.A.C.M. (2001), "Stability studies of ultra-long four span suspension bridge", *Proceedings of IABSE Conference on Cable-supported Bridges*, Seoul, August.

Luo, X.Y., Wang, D.L. and Chen, A.R. (2011), "The landscape design and form finding study of Taizhou Yangtze river highway bridge", *Proceedings of International Conference on Electric Technology & Civil Engineering*, Wuhan, China.

Nazir, C.P. (1986), "Multispan balanced suspension bridge", *J. Struct. Eng*., **112**(11), 2512-2527.

Ohshima, H., Sato, K. and Watanable, N. (1984), "Structural analysis of suspension bridges", *J. Bridge Eng*., **110**(3), 392-404.

Tan, Y.G., Gong, F. and Zhang, Z. (2009), "Analytical method for main cable configuration of two-span self-anchored suspension bridges", *Struct*. *Eng*. *Mech*., **32**(5), 701-704.

Torben, F. (2001), "Multi-span Suspension Bridges", *Steel Struct*., **1**, 63-73.

Yoshida, O., Okuda, M. and Moriya, T. (2004), "Structural characteristics and applicability of four-span suspension bridge", *J. Bridge. Eng*., **9**(5), 453-463.

Zhang, X.J. (2010), "Study of structural parameters on the aerodynamic stability of three-tower suspension bridge", *Wind Struct*., **13**(5), 471-485.

Zhang, L.W., Xiao, R.C. and Xia, R.J. (2011a), "Mechanical analysis and study on structural parameter of partially earth-anchored cable-stayed bridge part one: mechanical analysis", *Appl. Mech. Mater*., **44-47**, 1898-1905.

Zhang, L.W., Xiao, R.C. and Xia, R.J. (2011b), "Mechanical analysis and study on structural parameter of partially earth-anchored cable-stayed bridge part two: parametric study", *Appl. Mech. Mater*., **44-47**, 1906-1912.

Zhang, L.W. and Xia, R.J. (2011c), "The reasonable finished dead state research of partially earth-anchored cable-stayed bridge", *Adv. Mater. Res.*, **255-260**, 1319-1325.

Zhang, W.M., Ge, Y.J. and Levitan, M.L. (2011), "Aerodynamic flutter analysis of a new suspension bridge with double main spans", *Wind Struct*., **14**(3), 187-208.